Changing CO2 conditions during the end-Triassic inferred from stomatal frequency analysis on Lepidopteris ottonis (Goeppert) Schimper and Ginkgoites taeniatus (Braun) Harris

N.R. Bonis, J.H.A. Van Konijnenburg-Van Cittert, W.M. Kürschner

Palaeogeography, Palaeoclimatology, Palaeoecology 295 (2010) 146–161

Contents lists available at ScienceDirect

Palaeogeography, Palaeoclimatology, Palaeoecology

journal homepage: www.elsevier.com/locate/palaeo

Changing CO_2 conditions during the end-Triassic inferred from stomatal frequency analysis on *Lepidopteris ottonis* (Goeppert) Schimper and *Ginkgoites taeniatus* (Braun) Harris

N.R. Bonis [a,*], J.H.A. Van Konijnenburg-Van Cittert [a,b], W.M. Kürschner [a]

[a] Palaeoecology, Institute of Environmental Biology, Faculty of Science, Utrecht University, Laboratory of Palaeobotany and Palynology, Budapestlaan 4, 3584 CD Utrecht, The Netherlands
[b] Netherlands Centre for Biodiversity Naturalis, PO Box 9517, 2300 RA Leiden, The Netherlands

ARTICLE INFO

Article history:
Received 14 October 2009
Received in revised form 20 May 2010
Accepted 25 May 2010
Available online 1 June 2010

Keywords:
Triassic
Stomatal density
Stomatal index
Seedfern
Atmospheric CO_2
Palaeoclimate

ABSTRACT

End-Triassic fluctuations in atmospheric carbon dioxide (CO_2) concentration were reconstructed by the use of stomatal frequency analysis on a single plant species: the seedfern *Lepidopteris ottonis* (Goeppert) Schimper. Stomatal index showed no distinct intra- and interpinnule variation which makes it a suitable proxy for past relative CO_2 changes. Records of decreasing stomatal index and density from the bottom to the top of the Rhaetian–Hettangian Wüstenwelsberg section (Bavaria, Germany) indicate rising CO_2 levels during the Triassic–Jurassic transition. Additionally, stomatal frequency data of fossil ginkgoalean leaves (*Ginkgoites taeniatus* (Braun) Harris) suggest a maximum palaeoatmospheric CO_2 concentration of 2750 ppmv for the latest Triassic.

1. Introduction

The transition from the Triassic to the Jurassic period is characterized by large perturbations in organic carbon-isotope records (Pálfy et al., 2001; Hesselbo et al., 2002; Ruhl et al., 2009). These perturbations are related to changes in the global carbon cycle, and have often been linked to massive volcanic CO_2 input associated with the Central Atlantic Magmatic Province (CAMP), and/or methane hydrate release (Beerling and Berner, 2002; Hesselbo et al., 2002, 2007; Jenkyns, 2003). Additionally, degassing of organic rich shales and petroleum bearing evaporites as a result of widespread sill intrusion could have led to greenhouse gas and halocarbon generation in sufficient volumes to cause a negative carbon-isotope excursion (McElwain et al., 2005; Svensen et al., 2009).

The stomatal density (SD) and stomatal index (SI) of leaf cuticles are both inversely related to atmospheric CO_2 concentration during growth (e.g., Woodward, 1987; Kürschner et al., 1998) and can be used to reconstruct palaeoatmospheric CO_2 levels on short times scales (Beerling, 1993; McElwain et al., 1995; Wagner et al., 1999) and for deep time (Van der Burgh et al., 1993; McElwain et al., 1999, Royer et al., 2001a; Royer, 2001; Beerling, 2002b; Beerling et al., 2002; Retallack, 2001, 2009; Kürschner et al., 2008). Epidermal cell expansion can be influenced by e.g., sunlight intensity, water availability, salinity, and soil nutrient deficiency. Therefore, SI is a more sensitive parameter for detecting shifts in CO_2 concentration as it expresses stomatal frequency independently of variation in epidermal cell size (Van der Burgh et al., 1993; Kürschner, 1996; Kürschner et al., 1996; Beerling, 1999; Royer, 2001; Beerling and Royer, 2002a, 2002b). A fourfold increase (from 600 to 2100–2400 ppmv) of atmospheric CO_2 across the Triassic–Jurassic boundary was suggested based on stomatal frequency analysis (McElwain et al., 1999). On the other hand, carbon-isotope compositions of pedogenic calcite from paleosol formations indicate relative stability of atmospheric CO_2 (a rise of 250 ppmv) across the boundary (Tanner et al., 2001). These contrasting results could have been caused by differences in temporal resolution, i.e. stratigraphic spacing of samples (Beerling, 2002a). Furthermore, the suitability of the pedogenic-isotopic palaeobarometer may be questioned because of the compromising effect of massive dissociation events from methane hydrate reservoirs (Retallack, 2002a). The advantage of stomatal frequency records over other CO_2 proxies is that the SI of leaves responds immediately to CO_2 change (e.g., Wagner et al., 1996), which makes this parameter ideal for detecting rapid fluctuations (Wagner et al., 1999; Royer et al., 2001b; McElwain et al., 2005; Wagner et al., 2005). The Triassic–Jurassic boundary study by McElwain et al. (1999) was based on a mixed selection of ginkgoalean and cycadalean species. Because the SI is species specific (Kürschner et al., 1996;

* Corresponding author.
E-mail address: n.r.bonis@uu.nl (N.R. Bonis).

0031-0182/$ – see front matter © 2010 Elsevier B.V. All rights reserved.
doi:10.1016/j.palaeo.2010.05.034

Royer, 2001; Roth-Nebelsick, 2005; Retallack, 2009) it would be advantageous to examine a section with the same species occurring in several stratigraphic layers.

In order to detect changes in the end-Triassic atmospheric CO_2 regime, a stomatal frequency analysis of a temporal leaf record of a single plant species, *Lepidopteris ottonis* (Goeppert) Schimper, is presented. Leaves of this seed fern were collected from a series of successional organic rich layers exposed in the Rhaetian–Hettangian Wüstenwelsberg quarry (Bavaria, southern Germany). The minimal amount of fields of view was investigated before using this species as a proxy for relative CO_2 changes. Furthermore, the intra- and inter-pinnule variabilities of the stomatal frequency parameters were investigated in detail. These factors are important to know for the reliability of measurements from smaller pinnule fragments because often only small fragments are available in the fossil record. The uppermost macrofossil layer contains both *L. ottonis* and *Ginkgoites taeniatus* (Braun) Harris. By using modern *Ginkgo biloba* as 'nearest living equivalent,' stomatal frequency data of the latter species enable a quantitative CO_2 estimate for the latest Triassic.

2. Materials and methods

2.1. The Wüstenwelsberg quarry

The studied section is located in a quarry near the village of Wüstenwelsberg, Germany (Fig. 1). The sediments were deposited in the Germanic Basin and are characterized by an alternation of clay and sandstone layers (Fig. 2). The stratigraphic succession was sampled at three different locations within a few metres distance from each other. The base of each succession is indicated with a 0 in the lithological column (Fig. 2). The lowermost part of the section consists of an organic rich clay layer (1) with very abundant *Lepidopteris ottonis* leaves. This layer is followed by a thick sandstone (the 'Hauptsandstein'), which probably belongs to the Postera beds (Ruhl, 2010). On top of the sandstone lies a ~1 m thick interval with alternating clay and sandstone layers. Some *L. ottonis* specimens were found in this interval (1a). The consecutive sandstone (~1.5 m thick) is followed by a 10 m thick clay interval ('Hauptton') which represents the middle Rhaetian Contorta beds (Ruhl, 2010). The clay interval contains several fossil layers (k2c,

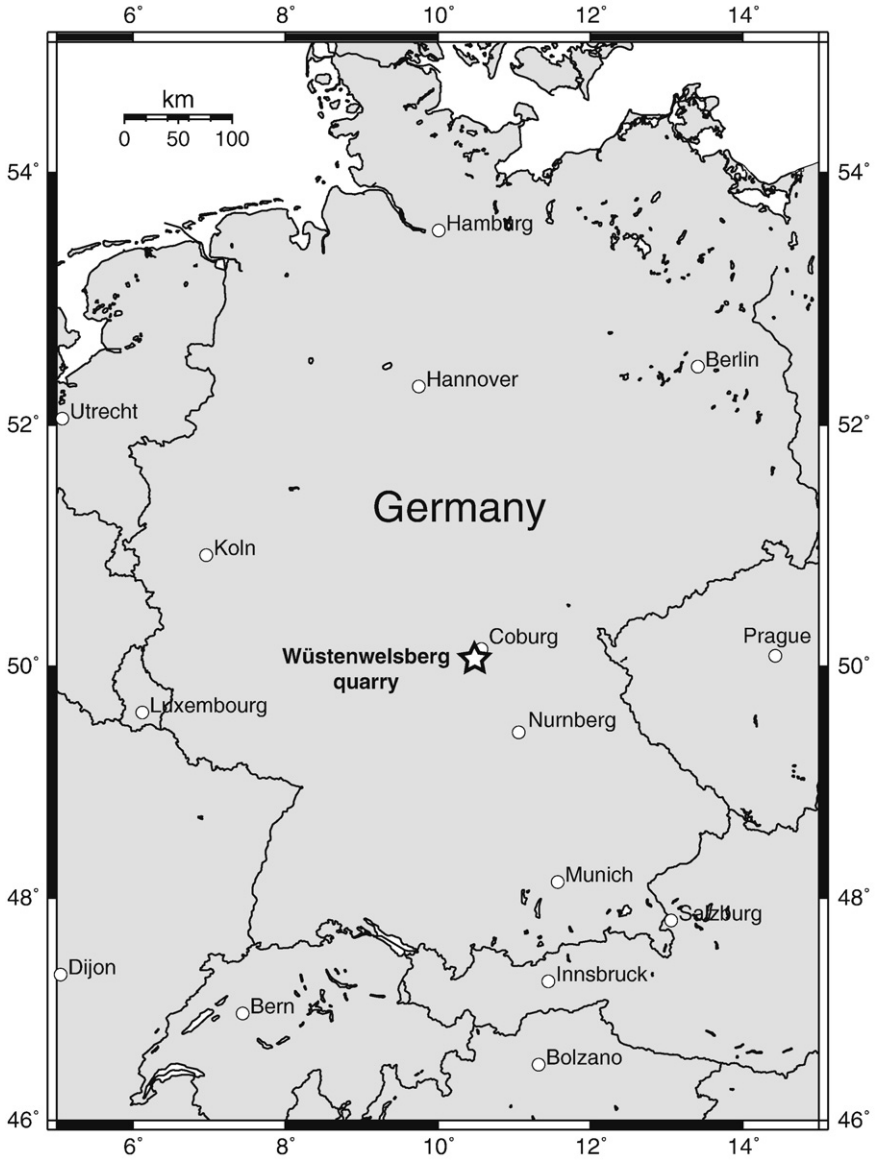

Fig. 1. Present-day location of the studied section, the coordinates of the Wüstenwelsberg quarry are 50°08′N/10°48′E.

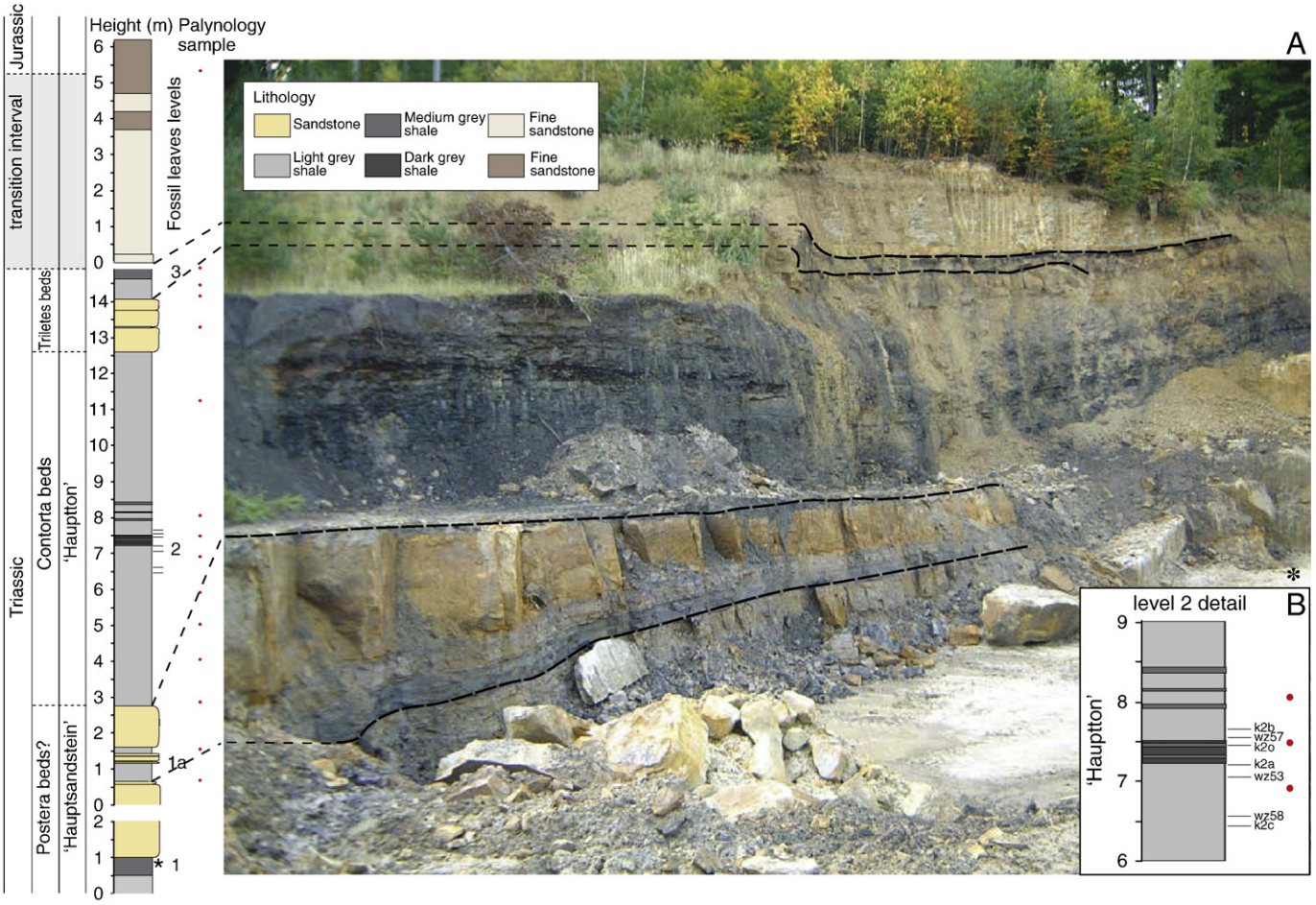

Fig. 2. A) Lithology of the Wüstenwelsberg section, position of the fossil levels and position of the palynology samples. For practical reason, three different locations within a few metres distance from each other were chosen for sampling. The base of each location is indicated with a 0 in the lithological column. The asterisk indicates the position where a hole was excavated to sample the lowermost clay layer with abundant *Lepidopteris ottonis* leaves. B) Detail of level 2 with the position of all the layers.

wz58, wz53, k2a, k2o, wz57 and k2b, together indicated as level 2, Fig. 2B) with a diverse macroflora, including *L. ottonis*. Occasionally, coal seams and large pyrite nodules are present. On top of the clays lies another sandstone (~1.5 m thick) followed by the uppermost organic rich clay layer (3) of the section. This interval belongs to the upper Rhaetian Triletes beds (Ruhl, 2010) and contains a more diverse macroflora than the Hauptton. *Ginkgoites taeniatus* is by far the most dominant species and rare *L. ottonis* leaves have been found.

2.2. Description of the fossil leaf material

The fossil leaf material used in this study partly originates from fieldtrips by the authors, and partly from the private collections of Stefan Schmeissner (Kulmbach, Germany) and Günter Dütsch (Untersteinach, Germany).

2.2.1. *Lepidopteris ottonis (Goeppert) Schimper, 1869*

Lepidopteris ottonis belongs to the Peltaspermales (Pteridospermopsida, Gymnospermae) and was morphologically and taxonomically described from Sweden (Antevs, 1914; Lundblad, 1950), East Greenland (Harris, 1926; 1932), Poland (Barbacka, 1991), and Germany (Schimper, 1869; Kelber and Van Konijnenburg-Van Cittert, 1997). Fig. 3A shows a *L. ottonis* specimen from the lowermost fossil level in the Wüstenwelsberg quarry. In the scope of this study only the main characteristics of the cuticle are discussed (Fig. 3C and E). The upper leaf surface is thicker than the lower leaf surface. Cuticularisation is strong, but the degree of cuticularisation varies between different pinnule cuticles. The epidermal cells have a polygonal, at times somewhat oblong shape with thick straight walls and occasionally sinuous extensions. Cells are more rectangular over the veins. Papillae in the middle of the epidermal cells are usually present. Stomata are irregularly distributed on both cuticle surfaces (amphistomatic), but are far more numerous on the lower one. Occasionally, they are present over the veins. The stomata have 4–7 (mostly irregular) subsidiary cells with papillae on top covering the stomatal aperture and sunken guard cells. Two adjacent stomata are common and even three adjacent stomata have been found. It was already mentioned by Harris (1926 p. 69) that "the great majority of the stomata are in fact somewhat irregular."

2.2.2. *Ginkgoites taeniatus (Braun) Harris, 1935*

Ginkgoites taeniatus belongs to the Ginkgoales (Gymnospermae) and was morphologically and taxonomically described from East Greenland (Harris, 1935). Fig. 3B shows fragments of *G. taeniatus* leaves from the uppermost fossil level (3) in the Wüstenwelsberg quarry. The cuticle is thicker on the upper side and it shows slightly elongated or isodiametric cells with straight walls (Fig. 3F). Papillae in the middle of the epidermal cells are absent. The cells along the veins are slightly more elongated. The stomata are irregularly distributed over the surface. Subsidiary cells have large papillae overhanging the stomatal pore. The thinner lower cuticle (Fig. 3D) has isodiametric cells between the veins which are elongated. The epidermal cell walls are nearly straight. Papillae on the epidermal cells are usually absent. Stomata are confined to interveinal bands. The guard cells are sunken and surrounded by about five subsidiary cells which sometimes have overhanging papillae.

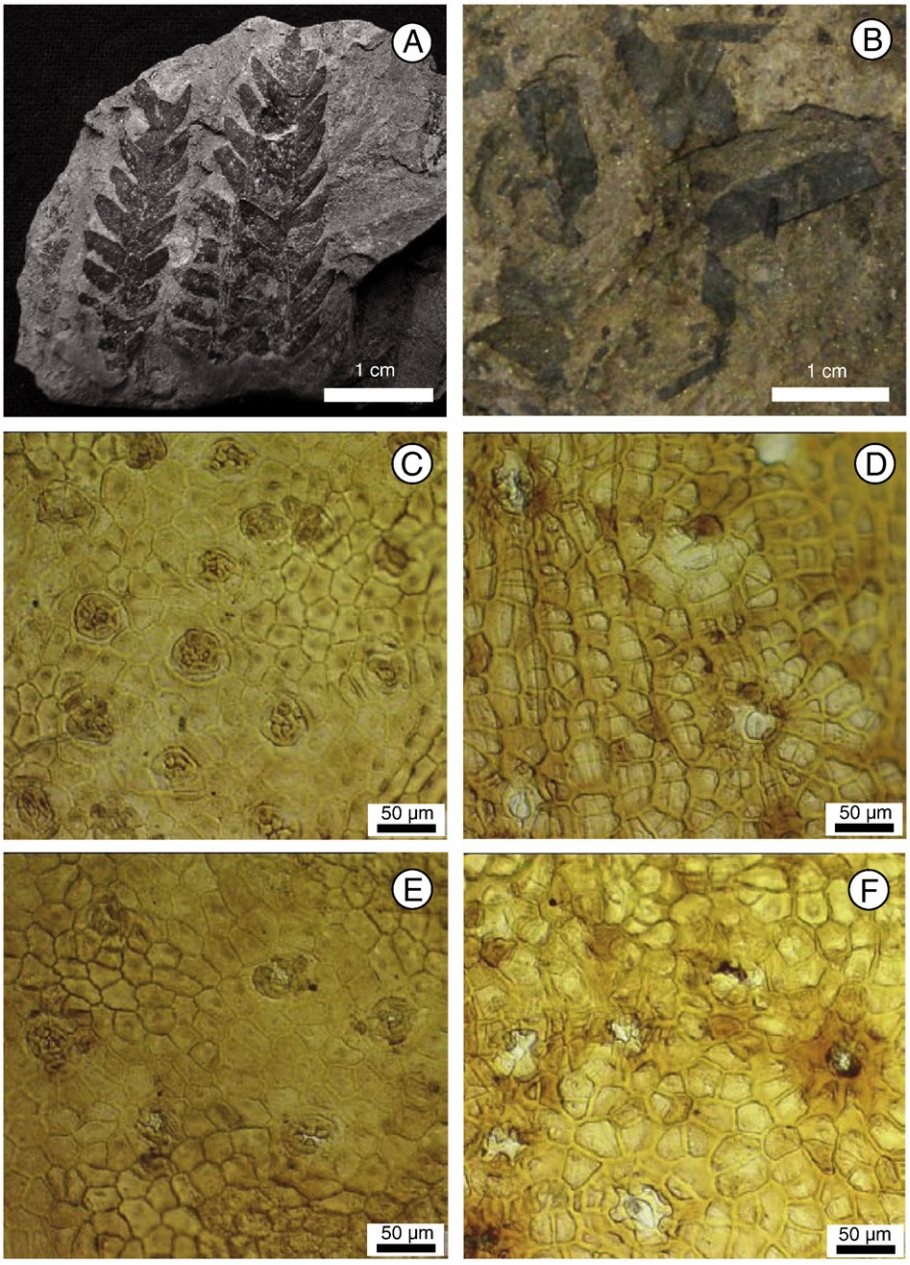

Fig. 3. A) A *Lepidopteris ottonis* leaf from level 1. B) Fragments of *Ginkgoites taeniatus* leaves from level 3. C) Abaxial cuticle surface of *Lepidopteris ottonis* from level 1, slide 1-A-A. D) Abaxial cuticle surface of *Ginkgoites taeniatus* from level 3, slide Gi-3-A. E) Adaxial cuticle surface of *Lepidopteris ottonis* from level 1, slide 1-A-A. F) adaxial cuticle surface of *Ginkgoites taeniatus* from level 3, slide Gi-3-A.

2.3. Maceration technique

Cuticles were picked directly from the rock surface. They were macerated according to the standard procedure (e.g., Kerp, 1990) using Schulze's reagent (30% HNO_3 with a few $KClO_3$ crystals) and subsequently treated with 5–10% potassium hydroxide (KOH). Macerated cuticles were rinsed with water. The upper and lower cuticle surface were separated and embedded in glycerine jelly on microscopic slides. The slides are stored in the collection of the Section Palaeoecology, Laboratory of Palaeobotany and Palynology, Utrecht University.

2.4. Stomatal frequency analysis

Stomatal frequency is conventionally expressed in terms of stomatal density (SD) and stomatal index (SI). SD is the number of stomata per unit leaf area. SI is the number of stomata expressed as a percentage of the total number of cells. SI (%) was calculated after Salisbury (1927): $SI = [SD/(SD + ED)] * 100$. ED is the epidermal cell density per unit leaf area. SD and ED were measured on the abaxial (lower) side of the leaf with a magnification of 330× and a field of view as large as possible of 0.1287 mm^2. The abaxial side was measured because this side contains far more stomata than the adaxial side (Fig. 3C and E, see also Vörding, 2008). In contrast to the SD, SI expresses stomatal frequency independently of variation in epidermal cell size. Epidermal cell expansion can be influenced by e.g. sunlight intensity, water availability, salinity, and soil nutrient deficiency. Therefore, SI is a more sensitive parameter for detecting shifts in CO_2 concentration (Van der Burgh et al., 1993; Kürschner, 1996; Kürschner et al., 1996; Beerling, 1999; Royer, 2001; Beerling and Royer, 2002a,b). The 'stomatal ratio method' was applied to reconstruct CO_2 values. In this method, a 'nearest living equivalent' (NLE) is used, defined as an extant species which is, as far as possible, of comparable ecological setting and/or structural similarity to

Table 1
Species list of macrofossils found in the Wüstenwelsberg section, based on the finds by Stefan Schmeissner, Günter Dütsch and the authors.

Species	Affinity	Remarks
Level 3		
Dorycycadolepis	Cycads, Cycadales	Bracts
cf. *Pseudoctenis* sp.	Cycads, Cycadales	
Ctenis sp.	Cycads, Cycadales	
Nilssonia pterophylloides	Cycads, Cycadales	
Nilssonia sp.	Cycads, Cycadales	Broad leaves
Anomozamites spp.	Cycadophyta, Cycadeoidales/Bennettitales, Williamsoniaceae	At least 2 species
Pterophyllum cf. *tietzei*	Cycadophyta, Cycadeoidales/Bennettitales, Williamsoniaceae	
? *Otozamites*	Cycadophyta, Cycadeoidales/Bennettitales, Williamsoniaceae	
Dictyophyllum cf. *nilssonii*	Ferns, Filicales, Diperidaceae	
Clathropteris meniscoides	Ferns, Filicales, Dipteridaceae	
Thaumatopteris brauniana	Ferns, Filicales, Dipteridaceae	
Phlebopteris angustiloba	Ferns, Filicales, Mationiaceae	
Phlebopteris muensteri	Ferns, Filicales, Mationiaceae	
Cladophlebis spp.	Ferns, Osmundales, Osmundaceae	
Ginkgoites taeniatus	Ginkgophyta, Ginkgoales	Frequent
Schmeissneria sp.	Ginkgophyta, Ginkgoales	
Equisetites sp.	Horsetails, Equisetales	
Pachypteris sp.	Seed ferns, Corystospermales	
Lepidopteris ottonis	Seed ferns, Peltaspermales	Rare
Peltaspermum sp.	Seed ferns, Peltaspermales	Female fructification Lepidopteris
Ctenozamites wolfiana	Seed ferns	
Ptilozamites heeri	Seed ferns	
cf. *Rhaphidopteris* sp.	Seed ferns	
Stachyotaxus elegans	Coniferales, Palissyaceae	
Elatocladus sp.	Coniferales	
Cones	Coniferales	
Needles	Conifers? or Czekanowskiales?	
Taeniopteris sp.	Probably Cycadophyta	Leaf morphogenus
Selaginella sp.	Lycophytes, Selaginellales	
Level 2		
Anomozamites	Cycads, Cycadeoidales/Bennettitales, Williamsoniaceae	
Dictyophyllum cf. *nilssonii*	Ferns, Filicales, Diperidaceae	
Phlebopteris muensteri	Ferns, Filicales, Mationiaceae	
Spiropteris sp.	Ferns	
Equisetites sp.	Horsetails, Equisetales	
Lepidopteris ottonis	Seed ferns, Peltaspermales	
Seed fern	Seed ferns	
Level 1a		
Stachyotaxus elegans	Conifers	
Lepidopteris ottonis	Seed ferns, Peltaspermales	
Level 1		
Stachyotaxus elegans	Conifers	
Dictyophyllum cf. *nilssonii*	Ferns, Filicales, Diperidaceae	
Phlebopteris muensteri	Ferns, Filicales, Mationiaceae	
Todites sp.	Ferns, Osmundales, Osmundaceae	
Lepidopteris ottonis	Seed ferns, Peltaspermales	Frequent
Peltaspermum sp.	Seed ferns, Peltaspermales	Female fructification Lepidopteris
Antevsia sp.	Seed ferns, Peltaspermales	Male fructification Lepidopteris
Seed fern	Seed ferns	
Cones	Coniferales	
Needles	Conifers	

its fossil counterpart (McElwain and Chaloner, 1995). The stomatal ratio (SR) was calculated by dividing the SI of the NLE by the SI of the fossil. McElwain and Chaloner (1995) standardized the stomatal ratios of Late Carboniferous conifers against CO_2 estimates based on a long term C cycle model (McElwain et al., 1999). With the use of this Carboniferous standard, 1 SR = 2 RCO_2 = 600 ppm CO_2 (McElwain 1998; McElwain et al., 1999), maximum CO_2 values were calculated. RCO_2 is the ratio of atmospheric CO_2 concentration estimated from stomatal ratios relative to a preindustrial value of 300 ppm (McElwain et al., 1999). Minimum CO_2 values were calculated using the Recent standard, where 1 SR = 1.2 RCO_2 = 360 ppm CO_2 (McElwain 1998; McElwain et al., 2005).

2.5. Palynology

Twenty-one palynological samples from the Wüstenwelsberg section were selected for palynological analysis. Between 5 and 20 g of sediment was crushed into small fragments and dried for 24 h at 60 °C. Subsequently, the samples were treated twice alternately with cold HCl (30%) and cold HF (40%) to remove the carbonates and silicates. The residues were sieved using a 250 μm and a 15 μm mesh. $ZnCl_2$ was applied to separate the lighter organic material from the heavier mineral particles. The lighter fraction was transferred from the test-tube and sieved once more using a 15 μm mesh. The remaining organic material was mounted on two slides per sample with glycerine jelly. The slides are stored in the collection of the Section Palaeoecology, Laboratory of Palaeobotany and Palynology, Utrecht University.

3. Results

3.1. The age of the Wüstenwelsberg section

The fossil layers in the Wüstenwelsberg quarry contain a diverse end-Triassic flora (Table 1). The upper level has the most diverse flora and is dominated by *Ginkgoites taeniatus* (Table 1). *Lepidopteris*

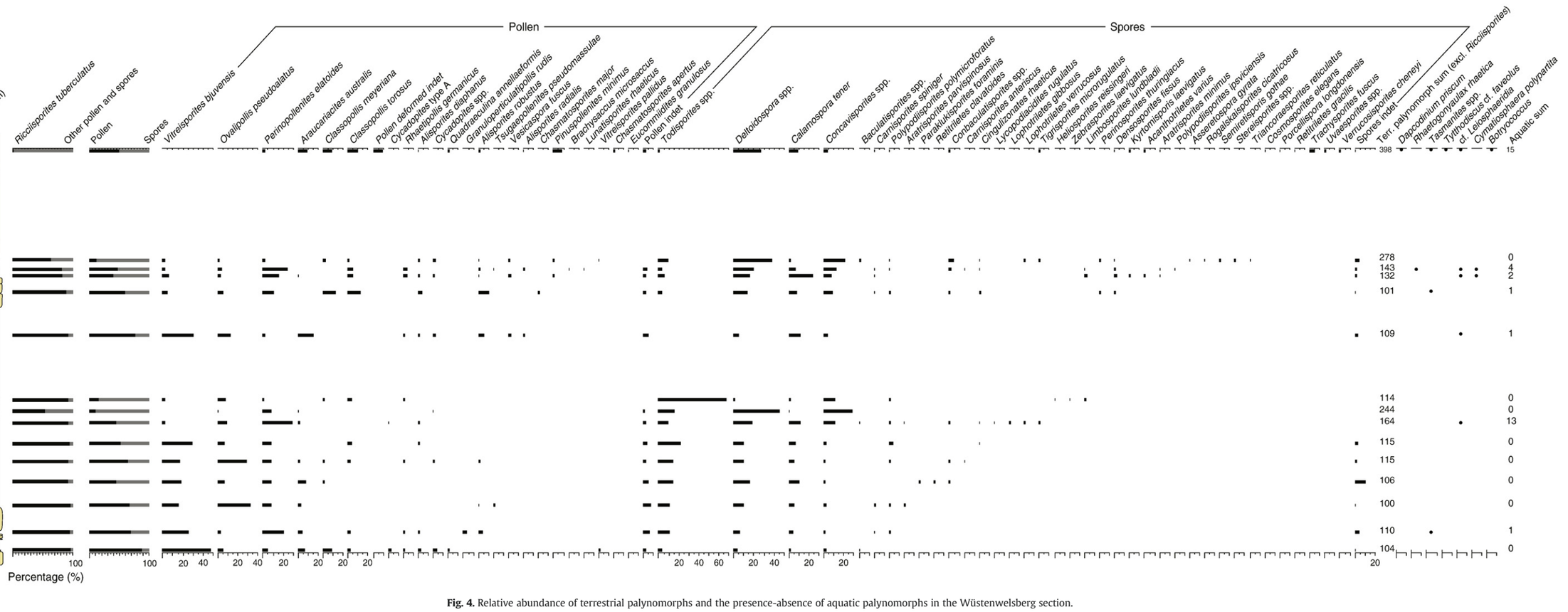

Fig. 4. Relative abundance of terrestrial palynomorphs and the presence-absence of aquatic palynomorphs in the Wüstenwelsberg section.

ottonis, present in all levels, is restricted to the Rhaetian stage (Antevs, 1914; Barbacka, 1991; Kelber and Van Konijnenburg-Van Cittert, 1997). In East Greenland, sediments from the Rhaetian and the Lower Jurassic are part of the *Lepidopteris* zone and the *Thaumatopteris* zone, respectively (Harris, 1935; McElwain et al., 1999, 2007). The family of *L. ottonis* (Peltaspermaceae) went extinct at the Triassic–Jurassic boundary (e.g., Ash, 1986). The conifer *Stachyotaxus elegans* (Table 1) is also characteristic of the Rhaetian stage (Kelber and Van Konijnenburg-Van Cittert, 1997). In East Greenland, *G. taeniatus* is characteristic of the lower and middle part of the Hettangian *Thaumatopteris* zone (Harris, 1935).

Fifteen out of the twenty-one palynological samples were productive (Figs. 2, 4). *Ricciisporites tuberculatus* dominates (>95%) most of the samples and is therefore shown separate from the other pollen and spores (Fig. 4). From the base up to 15 m, the most abundant pollen types are *Vitreisporites bjuvensis*, *Ovalipollis pseudoalatus* and *Perinopollenites elatoides*. Persistent spore types are *Todisporites* spp., *Deltoidospora* spp., *Calamospora tener* and *Concavisporites* spp. The amount of spores is highest in the darker organic rich layers. Based on the abundance of *V. bjuvensis*, *Ovalipollis pseudoalatus* and the presence of *Rhaetipollis germanicus*, *Lunatisporites rhaeticus* and *Rhaetogonyaulax rhaetica* the samples up to 15 m in the section are assigned to the end-Triassic. In the uppermost palynological sample from Wüstenwelsberg *R. tuberculatus* is almost absent. This sample consists of 50% pollen with *Classopollis meyeriana*, *Classopollis torosus*, *Araucariacites australis*, *Pinuspollenites minimus* and unidentified deformed pollen as the most abundant elements. Most likely, the deformed pollen belongs to *Classopollis* but it is not possible to distinguish between *C. meyeriana* and *C. torosus*. Most abundant spore taxa are *Deltoidospora* spp., *Calamospora tener*, *Trachysporites fuscus* and *Concavisporites* spp. Remarkable is also the presence of 5% aquatic palynomorphs, mainly consisting of the dinoflagellate cyst *Dapcodinium priscum*. The higher abundance of *P. minimus*, *T. fuscus*, *D. priscum* and the absence of *V. bjuvensis*, *Ovalipollis pseudoalatus*, *R. germanicus*, *Lunatisporites rhaeticus* and *Rhaetogonyaulax rhaetica* suggests an early Jurassic age of this sample. The difference between the lower palynomorph assemblages and the one above fossil level 3 is similar to the difference between Triassic and Jurassic assemblages from the Eiberg Basin in Austria (Kuerschner et al., 2007; Bonis et al., 2009). Despite the presence of *Ginkgoites taeniatus*, which occurs in the lower Jurassic in East Greenland, it appears that levels 1, 1a, 2 and 3 are all end-Triassic in age based on the palynological record. This is confirmed by the carbon-isotope stratigraphy (Ruhl, 2010).

3.2. Number of counted fields of view of *Lepidopteris ottonis* and *Ginkgoites taeniatus* cuticles

Relatively stable SI values for one *Lepidopteris ottonis* pinnule were derived after counting seven fields of view (Fig. 5A) of 0.1287 mm^2. An exception is pinnule WZ53-A-A, which still shows gradually decreasing values after seven fields. Another pinnule from this level (WZ53-B-A) does show stable values after six fields. Unfortunately it was not always possible to count a minimum of seven fields. Parts of the pinnule surface are unreliable for measurements due to the presence of veins or damage of the cuticle. Stable SI values for one *Ginkgoites taeniatus* leaf were obtained after counting ten fields of view (Fig. 5B). For both species, the standard deviations of the SI values were low, e.g., a mean of 0.71 for *L. ottonis* and a mean of 0.57 for *G. taeniatus*.

3.3. Intrinsic leaf variability in *Lepidopteris ottonis*

It is important to investigate the intra- and interpinnule variation of the ED, SD and SI for the reliability of measurements from smaller pinnule fragments. The ED, SD and SI were measured at different positions on a pinnule from level 1 (Fig. 6A) and level 3 (Fig. 6B). The SI and SD decrease and the ED increases from the base to the apex in pinnule 1-A-A while in pinnule 3-A-A all parameters increase from the base to the apex. Although there are differences in the mean SD, ED and SI for the apex, middle and base of both pinnules this seems to be arbitrary as there is a different pattern in both pinnules. Exceptionally higher or lower SI values occur at all positions of the pinnules. For example, the lowest SI values from pinnule 3-A-A are located at the base edge (2.52) as well as in the middle closer to the midrib (2.98). There is no pattern in fields of view close to the margin or close to the midrib. It seems that the measurements just capture the natural variability in a pinnule. However, to get the most reliable SI for one pinnule the whole pinnule should be counted, including positions on the apex, base and middle part of the pinnule.

The interpinnule variability is checked by measuring four different pinnules from the same leaf (Fig. 7A). There is no distinct variation in ED, SD or SI between different pinnules from the same leaf (Fig. 7B, C, D). This implies that analysing one pinnule per leaf is enough to obtain consistent ED, SD and SI values.

3.4. Temporal stomatal frequency trends

There is some variability in the ED, SD and SI between different leaves within one level (Table 2, Fig. 8). This is probably a reflection of the natural variability of a species. More important is that despite this variability, there are distinct differences in the SI (and SD and ED) throughout the record (Fig. 8). From level 1 to level wz58 there is a decreasing trend in the SI and SD. The ED decreases from level 1 to level 1a but remains stable from level 1a to level wz58. The subsequent levels (wz53, k2a and k2o) show higher SI values (Fig. 8). Important to note is that these levels are positioned the closest to the very high organic rich interval (Fig. 2). Level k2o, which is positioned within the darkest shales, shows distinctive higher SD and ED values (Fig. 8). Above level k2o, SI levels decrease towards the uppermost level 3. In addition, in level 3 stomatal frequency analysis was carried out on *Ginkgoites taeniatus* leaves. SD values are lower than for *Lepidopteris ottonis* and ED values are positioned within the lower range of the values from *L. ottonis*. This results in a lower SI (Fig. 8).

4. Discussion

4.1. Changes in the stomatal frequency analysis parameters

The intra- and interpinnule variation was checked before using the stomatal frequency of *Lepidopteris ottonis* as a proxy for palaeoatmospheric CO_2. The intrinsic variability of *L. ottonis* pinnules is very low (Figs. 6 and 7). The SI of *L. ottonis* from Scania also showed almost identical values for different parts of the pinnules (Vörding, 2008). Furthermore, the SI within a complete frond or frond portions is fairly stable justifying the use of SI values from *L. ottonis* as a proxy for CO_2 if this species is sensitive to CO_2 changes (Vörding, 2008). An overall decreasing trend in the SI and SD of *L. ottonis* is present from the bottom to the top of the studied section (Fig. 8). SI is inversely related to the ambient CO_2 concentration during growth and can therefore be used to reconstruct palaeoatmospheric CO_2 (Woodward, 1987; Kürschner, 1996; Kürschner et al., 1996; McElwain et al., 1999; Royer, 2001; Retallack, 2001, 2009). To exclude the effect of changing ED as the main driver of SI instead of a higher SD induced by higher CO_2 concentration, two SI simulations were carried out (Fig. 9A). The first one was calculating the SI with a constant mean ED value of 1410 n/mm^2. The second one was calculating the SI with a constant mean SD value of 78 n/mm^2. The simulated SI signal with constant ED values shows the same amplified pattern as the original SI record (Fig. 9A). This suggests that the changes in SD were indeed the main driver of changes in the SI. The uppermost SI value could be partly influenced by the strong increase in ED with respect to SD (Fig. 8). The

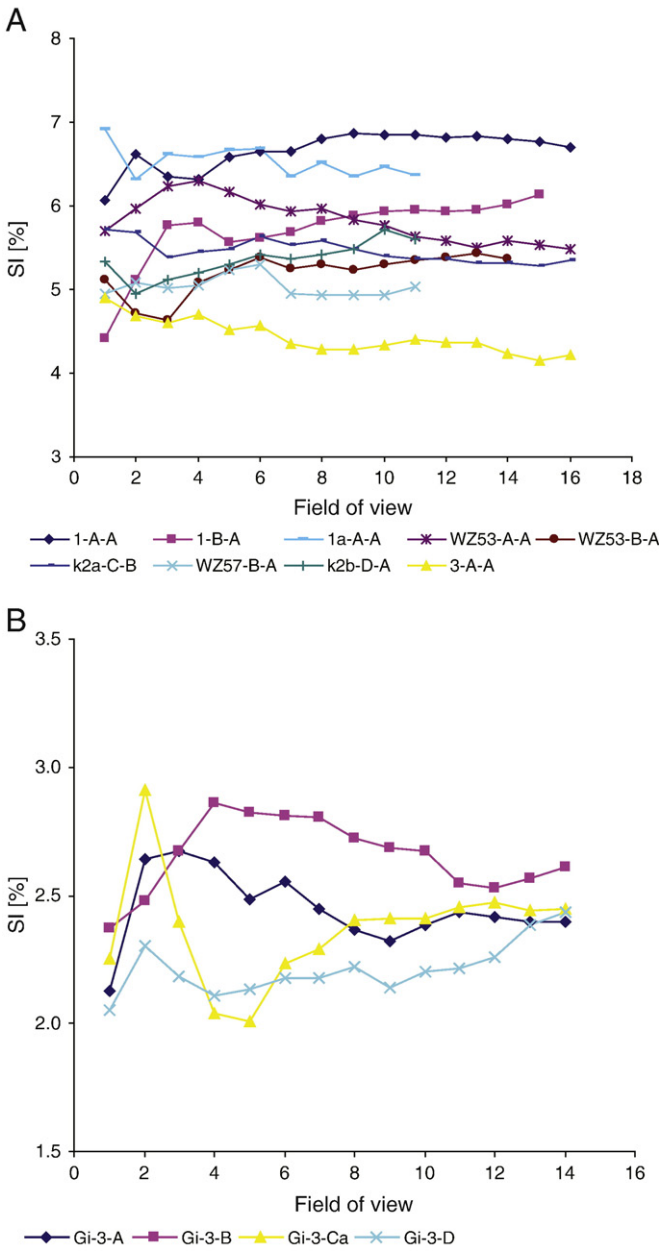

Fig. 5. A) Cumulative mean SI of *Lepidopteris ottonis*. B) Cumulative mean SI of *Ginkgoites taeniatus*.

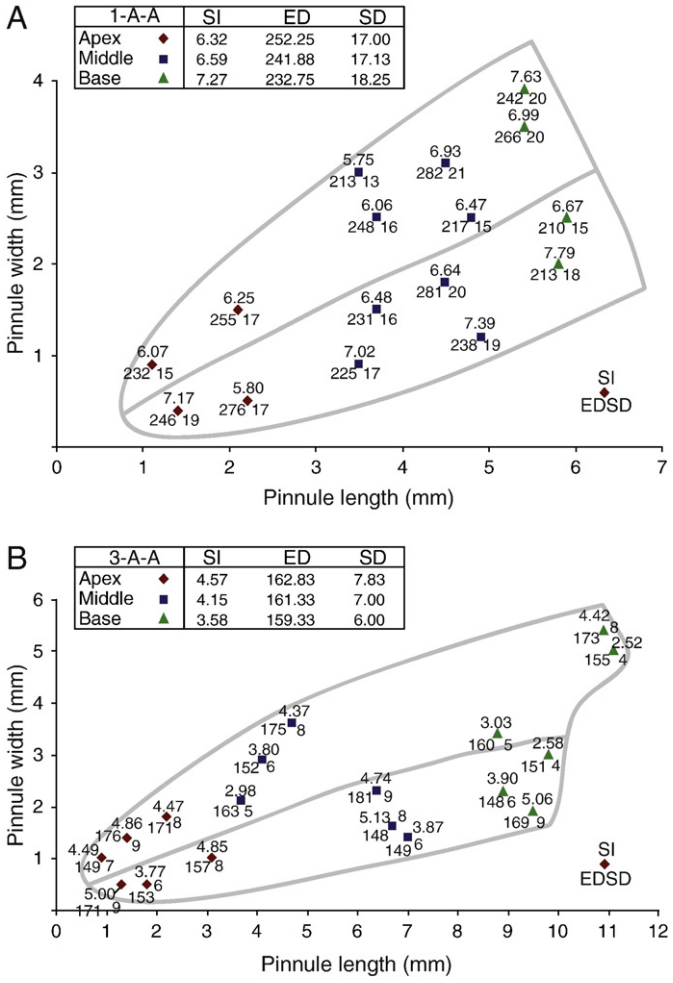

Fig. 6. A) Intrapinnule variation of a pinnule from level 1. B) Intrapinnule variation of a pinnule from level 3. ED and SD are indicated per field of view.

correlation between SD and ED is high ($R^2 = 0.74$) (Fig. 9B). This implies that if solely the SD was used to infer relative atmospheric CO_2 changes, the reconstructed CO_2 changes might be partly disturbed by ED, and consequently SD, changes related to changes in epidermal cell expansion caused by e.g. sunlight intensity, water availability, salinity, and soil nutrient deficiency. SI is preferable for a CO_2 reconstruction as there is a very low correlation ($R^2 = 0.14$) between SI and ED (Fig. 9D) and a higher correlation between SI and SD ($R^2 = 0.63$) (Fig. 9C). The lack of correlation between SI and ED implies that changes in SD rather than epidermal cell expansion were the cause for changes in the SI.

Lepidopteris ottonis might be a succulent, based on the strong cuticularisation (Antevs, 1914). In contrast, extraordinary thick cuticles are reported from *Lepidopteris callipteroides*, an early Triassic seed fern, but which lived in a humid environment (Retallack, 2002b). Another pronounced feature of *L. ottonis* are the papillae covering the stomata, speculated to be a mechanism for reducing transpiration in drought-prone soils (Retallack, 2002b). However, papillae overarching the stomata, sunken stomata and other xeromorph characteristics may also indicate adaptation to stress factors other than just a dry climate (Haworth and McElwain, 2008; Pott et al., 2008). One suggestion is that the papillae were helpful in reducing transpiration in soils low in nutrients (peinomorphic adaptation) (Retallack, 2002b). Physiological drought may also be caused by strongly permeable or osmotic soils, wind exposure, saline environments, low pH values, or an epiphytic way of life (Pott et al., 2008). McElwain et al. (2007) suggested that *L. ottonis* had a vine- or liana-like way of living based on similar anatomical and morphological characteristics common to among modern angiosperm vines and lianas (Krings et al., 2003). There are no indications to confirm this interpretation from the Wüstenwelsberg quarry specimens. The presence of papillae can be a way of preventing the formation of a water film on the leaf surfaces, which can adversely affect the uptake of CO_2 (Pott et al., 2008; Haworth and McElwain, 2008). Additionally, papillae can be helpful in the self-cleaning effect of the leaves with regard to dust, or atmospheric particles caused by local volcanism (Pott et al., 2008; Haworth and McElwain, 2008). A late Carnian flora from Lunz also showed adaptations (sunken stomata, papillate surfaces) to ecological conditions characteristic of peat swamps, e.g., physiological drought (Pott et al., 2008). Level k2o is positioned within the darkest organic rich shales and it shows distinctively higher SD and ED values (Fig. 8). Experimental leaves grown under high humidity levels show a lower SD and ED, caused by an increased cell expansion (Kürschner, 1996). Stomata can be packed more densely because of drought (e.g.,

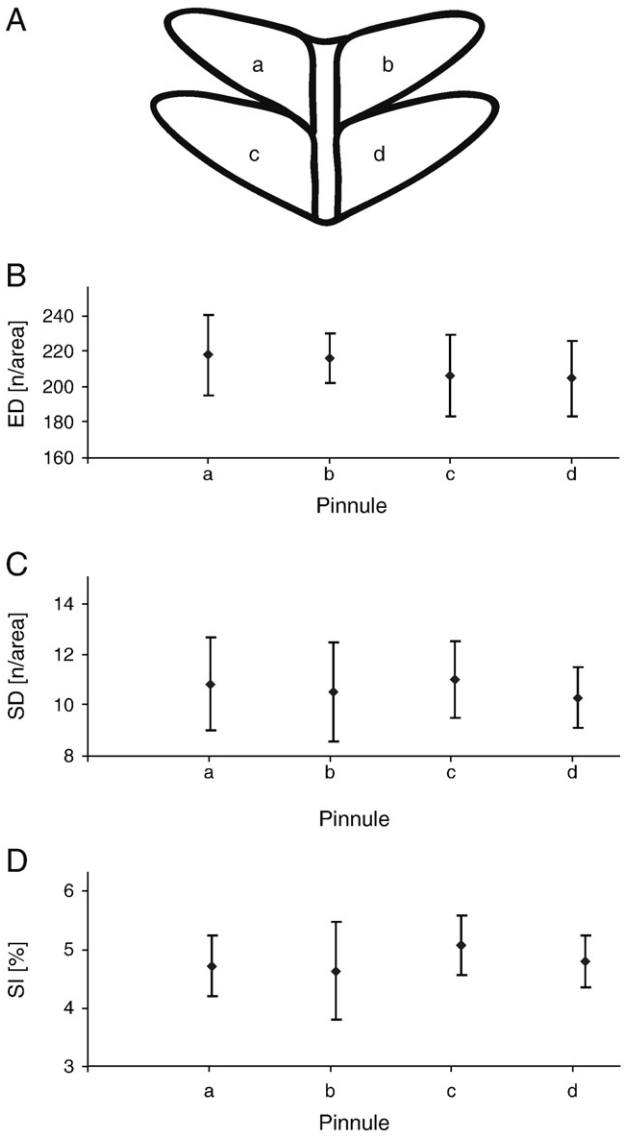

Fig. 7. A) Schematic representation of a measured leaf from level 2. B) Interpinnule variation of ED. C) Interpinnule variation of SD. D) Interpinnule variation of SI. Please note that the measurements are from a previous lower resolution study of level 2 and therefore the ED, SD and SI values are not included in Table 2. ED and SD values are indicated per field of view. The error bars represent the standard deviations.

Woodward, 1987; Royer, 2001). Leaves from this level show strongly cutinized cell walls and papillae in the middle of the epidermal cells. The high SD and ED in level k2o are probably the result of adaptation to a stressed environment. Probably, *L. ottonis* from Wüstenwelsberg had these xeromorph features because it lived in a humid and coal-producing swampy environment low in nutrients, rather than a dry environment. The palynological content of the organic rich samples confirms our interpretation of a swampy environment as fern spores are the major constituent of the assemblages.

4.2. Reconstruction of palaeoatmospheric CO_2

A comparison of our data with those published by Retallack (2001, 2009) appears to be of limited use as the age assessment of his data is rather vague. Moreover, stomatal counts have been made from previously published photographs which may be biased because of selection for good visibility of the epidermal cell patterns but are not necessarily representative for the stomatal density patterns of the fossil leaf material. The SI of *Lepidopteris ottonis* ranges between 6.3%

Table 2
Stomatal frequency analysis data from *Lepidopteris ottonis* and *Ginkgoites taeniatus* fossils found in the Wüstenwelsberg section.

Level	Depth (cm)	Slide (level-leaf-pinnule)	*n* areas	ED	ED sd	SD	SD sd	SI	SI sd
Lepidopteris ottonis									
1	Below SST	1-A-A	16	1882.31	189.64	135.04	17.92	6.70	0.62
		1-B-A	15	1884.48	112.51	123.32	19.89	6.13	0.85
		1-C-C	11	1726.12	146.25	106.69	15.58	5.83	0.73
		1-D-A	12	1785.00	88.88	117.88	11.87	6.20	0.60
Average 1			*54*	*1819.48*	*134.32*	*120.73*	*16.32*	*6.21*	*0.70*
1a	115	1a-A-A	11	1331.15	148.77	90.44	18.81	6.36	1.07
		1a-C-A	7	1420.08	225.82	86.60	20.28	5.70	0.67
		1a-C-B	9	1616.60	128.12	93.27	10.28	5.47	0.64
		1a-C (average)	16	1518.34	176.97	89.93	15.28	5.59	0.66
		1a-D-A	4	1478.65	171.97	77.72	20.07	4.95	0.84
		1a-E-A (2 pinnules)	12	1200.79	71.04	66.06	9.66	5.21	0.68
Average 1a			*43*	*1382.23*	*142.19*	*81.04*	*15.95*	*5.53*	*0.81*
K2C	647	K2c-A-A	7	1174.70	59.43	62.18	8.97	5.02	0.65
		K2c-B-A	4	1369.84	204.00	68.01	21.40	4.65	0.86
		K2c-C-A	5	1706.76	165.38	66.84	6.95	3.78	0.34
Average K2C			*16*	*1417.10*	*142.94*	*65.67*	*12.44*	*4.49*	*0.62*
WZ-58	652	WZ-58-A-A	9	1261.67	89.46	57.86	12.95	4.36	0.75
		WZ-58-B-A	8	1436.87	99.22	67.03	10.94	4.44	0.53
Average WZ-58			*17*	*1349.27*	*94.34*	*62.45*	*11.95*	*4.40*	*0.64*
WZ-53	707	WZ-53-A-A	16	1250.83	73.87	72.86	13.27	5.48	0.79
		WZ-53-B-A	14	1243.54	91.76	71.06	13.24	5.37	0.72
		WZ-53-C-A	14	1199.13	147.86	67.17	15.12	5.26	0.71
		WZ-53-D-A	7	1286.84	108.33	69.95	18.50	5.10	0.93
Average WZ-53			*51*	*1245.08*	*105.45*	*70.26*	*15.03*	*5.30*	*0.79*
K2A	720	K2a-A-A	11	1329.74	123.84	70.66	15.33	5.04	0.92
		K2a-B-A	9	983.60	99.62	63.04	9.87	6.01	0.55
		K2a-C-B	16	1587.94	94.92	89.87	13.00	5.35	0.57
		K2a-D-A	10	1193.02	107.90	62.18	10.36	4.94	0.55
		K2a-E-A	12	1200.79	220.22	49.22	13.80	3.92	0.78
		K2a-E-B	7	1247.98	142.88	58.85	11.75	4.56	1.09
		K2a-E (average)	19	1224.39	181.55	54.03	12.77	4.24	0.93
Average K2A			*65*	*1263.74*	*121.56*	*67.95*	*12.27*	*5.11*	*0.71*
K2O	744	K2o-A-A	9	1519.02	112.43	80.31	17.38	5.02	0.97
		K2o-B-A	8	1469.90	141.15	79.66	18.92	5.10	0.79
		K2o-C-A	11	1393.33	141.28	84.79	17.54	5.70	0.74
		K2o-C-B	10	1479.03	112.69	89.38	7.55	5.71	0.38
		K2o-C (average)	21	1436.18	126.98	87.08	12.54	5.70	0.56
		K2o-D-A	7	1833.11	189.45	119.91	12.58	6.15	0.51
Average K2O			*45*	*1564.55*	*142.50*	*91.74*	*15.36*	*5.49*	*0.71*
WZ-57	753	WZ-57-A-A	11	1339.63	98.02	72.78	13.58	5.12	0.66
		WZ-57-B-A	11	1292.29	129.45	69.24	16.47	5.03	0.84
Average WZ-57			*22*	*1315.96*	*113.74*	*71.01*	*15.03*	*5.07*	*0.75*
K2B	763	K2b-A-A	5	1181.36	32.05	55.96	6.50	4.51	0.42
		K2b-B-A	7	1186.91	77.81	59.96	5.88	4.81	0.34
		K2b-C-A	8	1114.33	75.12	55.38	16.32	4.69	1.17
		K2b-D-A	11	1423.00	73.61	84.79	16.83	5.60	0.90
		K2b-E-A	9	1456.84	119.09	73.40	18.68	4.75	0.84
Average K2B			*40*	*1272.49*	*75.53*	*65.90*	*12.84*	*4.87*	*0.73*
3	1480	3-A-A	18	1252.61	87.54	53.97	13.45	4.10	0.85
		3-B-A	8	1640.89	184.36	77.72	17.63	4.50	0.74
		3-C-A	9	1858.40	148.31	102.76	15.92	5.23	0.67
		3-B/C (same leaf, average)	17	1749.64	166.33	90.24	16.77	4.87	0.70
		3-D-A	7	1544.43	73.15	73.28	11.75	4.51	0.58
		3-D-B	7	1372.33	74.12	58.85	7.58	4.10	0.36
		3-D (average)	14	1458.38	73.63	66.06	9.67	4.31	0.47
Average 3			*49*	*1486.88*	*109.17*	*70.09*	*13.30*	*4.43*	*0.67*
Ginkgoites taeniatus									
3	1480	Gi-3-A	14	1774.26	143.00	43.86	10.39	2.40	0.47
		Gi-3-B	14	1719.86	112.44	46.08	9.38	2.61	0.51
		Gi-3-Ca	14	1571.63	93.62	39.42	11.99	2.45	0.72
		Gi-3-D	14	1985.78	177.91	49.96	15.46	2.43	0.58
Average 3			*56*	*1762.88*	*131.74*	*44.83*	*11.80*	*2.47*	*0.57*

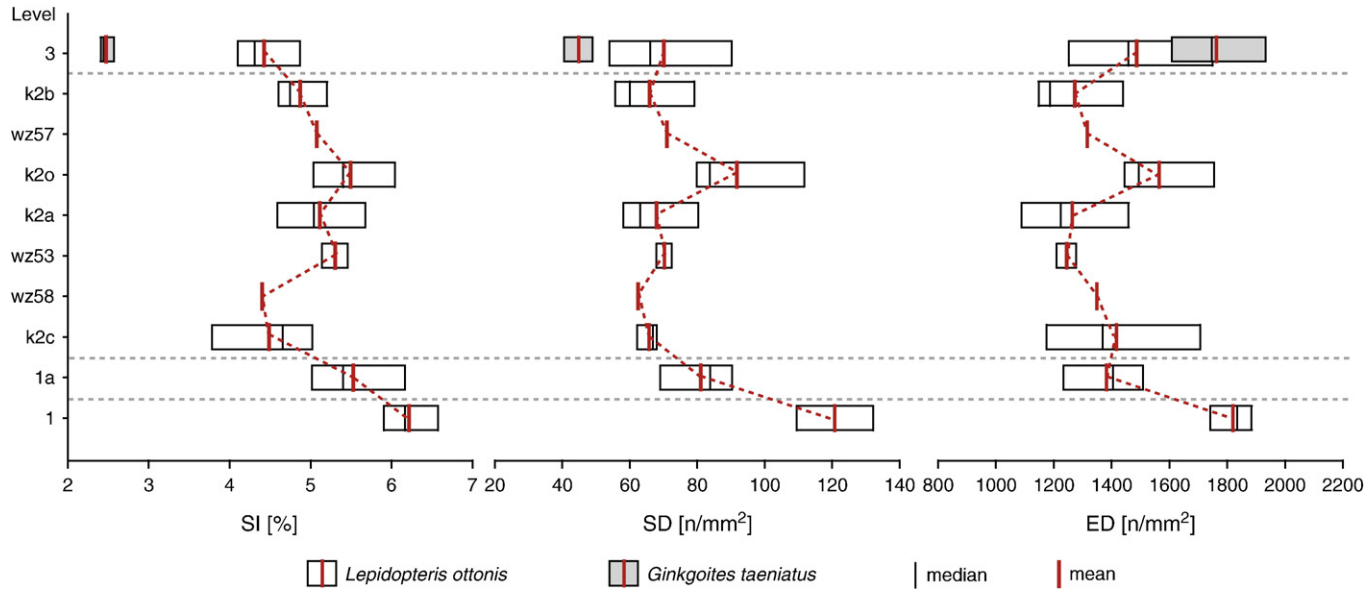

Fig. 8. Boxplots of the SI, SD and ED variations through the Wüstenwelsberg section. The dashed grey lines indicate that levels below and beneath are separated by a sandstone layer.

(±1.9) and 8.7%, comparable to the youngest sample from Wüstenwelsberg. The other SI values from Wüstenwelsberg are much lower than Retallack's values, which is also the case for *Ginkgoites taeniatus* with 2.47% versus 7.2%±0.5. If we apply our SI of *G. taeniatus* to the transfer functions based on ginkgoalean leaves obtained by Retallack (2001, 2009) unrealistic CO_2 values (respectively 7560 ppmv and 1,575,256 ppmv) are calculated. This is probably because our SI is outside the range of the calibrated SI values for the transfer functions. The functions appear to be incorrect for the low Triassic–Jurassic SI values. The same problem arises when using transfer functions proposed by Royer et al. (2001a); Beerling and Royer (2002a), and Royer (2003). Furthermore, these functions are more useful for the Cenozoic species, such as *G. occidentalis* and *Ginkgo biloba* (D.L. Royer, pers. comm., 2009). For these reasons we suggest that the stomatal ratio method (e.g., McElwain and Chaloner, 1995; McElwain et al., 1999, 2005) is the most appropriate for our fossil data.

Ginkgoalean leaves proved to be suitable for CO_2 reconstruction studies (McElwain et al., 1999; Chen et al., 2001; Retallack, 2001; Beerling and Royer, 2002b; Sun et al., 2008). The stomatal ratio (SR) was calculated by dividing the SI of the NLE by the SI of the fossil (Table 3a). We use *Ginkgo biloba* as the NLE of *Ginkgoites taeniatus* with an SI of 11.33% for a preindustrial CO_2 value of 300 ppm (McElwain et al., 1999). McElwain and Chaloner (1995) standardized the stomatal ratios of Late Carboniferous conifers against CO_2 estimates based on a long term C cycle model (McElwain et al., 1999). With the use of this Carboniferous standard, 1 SR = 2 RCO_2 = 600 ppm CO_2 (McElwain et al., 1999), a maximum CO_2 value of 2750 ppmv was reconstructed for level 3 (Table 3a; Fig. 10). When the recent standardization was used, 1 SR = 1.2 RCO_2 = 360 ppm CO_2 (McElwain, 1998; McElwain et al., 2005), a minimum CO_2 value of 1650 ppmv was reconstructed. Unfortunately, *Lepidopteris ottonis* has no NLE because the order to which it belonged (Peltaspermales) went extinct at the Triassic–Jurassic boundary (e.g., McElwain et al., 2007). However, in level 3 both *G. taeniatus* and *L. ottonis* are present together which means that at a maximum CO_2 value of 2750 ppmv *L. ottonis* had a SI of 4.43 (Table 3a). In order to infer CO_2 concentrations from *L. ottonis* in the lower part of the section the assumption was made that the difference between the SI from *G. taeniatus* and the SI from *L. ottonis* (1.95) maintained constant. The assumption that the slope in the SI–CO_2 response is the same for both species can only be confirmed if another stratigraphic layer is found where both species occur. Unfortunately, at present this is not the case. However, as there are no indications that the species have a completely different slope, we prefer to work with these values. With the corrected 'Ginkgoites' SI (SI '*Ginkgoites*' = SI *Lepidopteris* − 1.95) the relative changes in CO_2 were calculated (Table 3a, Fig. 10). Whereas the absolute values are estimates, it is obvious that there is a CO_2 increase (Fig. 10). Further work on species which do have a suitable NLE would certainly strengthen our understanding of absolute CO_2 changes during this time period.

An abrupt enigmatic CO_2 perturbation seems to occur in the middle of the Contorta beds (Fig. 10). One possibility is that this is a short term event with a drop in CO_2. However, there are no indications for such an event from the carbon-isotope record (Ruhl, 2010) or from other end-Triassic records. The question rises if the SI changes in this interval really reflect CO_2 dynamics. Therefore, the trends in SD were checked and in the lower part of the section a decline in SI from 6.2 to 4.4 ($\Delta CO_{2\ max}$ of 1182) is associated with a decline in SD from 121 to 62 (~50%). By contrast, the increase in SI in the Contorta beds from 4.4 to 5.3 ($\Delta CO_{2\ max}$ of 748) is only associated by an increase in SD from 62 to 70 (~10%). This decline in SD during the CO_2 increase is not proportional to the increase in SD during the CO_2 decrease of a similar order. The observed disproportion is caused by the changes in ED (Fig. 8) and therefore we assume that the SI changes in this part of the record do not reflect CO_2 changes. Because the ED is 10 to 20 times higher than SD, relative small changes in ED can cause large changes in the SI values. This ED sensitivity is a disadvantage when using SI values from *Lepidopteris ottonis* as a proxy for CO_2 changes. If we focus only on the regression between wz58 and wz53 (Fig. 9D) it is obvious that this would give a different regression line between ED and SI (i.e. ED would increase when SI decreases, dashed oval in Fig. 9D). This confirms that ED is indeed an influencing factor of the SI change between sample wz58 and wz53. To correct for the changes in ED, we reconstructed new CO_2 values for samples wz53 to 3 standardized on the changes in SD and CO_2 between level 1 and wz58 (Tables 3b and 3c). This combined SI/SD reconstruction (Fig. 10) still shows one outlier: sample k2o from the dark organic rich shales. The SI fluctuations in the organic rich layer can be influenced by a local stressed swamp environment (increased SD and ED) rather than a global CO_2 signal caused by CAMP volcanism and/or methane hydrate. A study on stomatal responses of modern *Polystichum munitum* (sword fern) growing near the Kilauea volcano on Hawaii showed

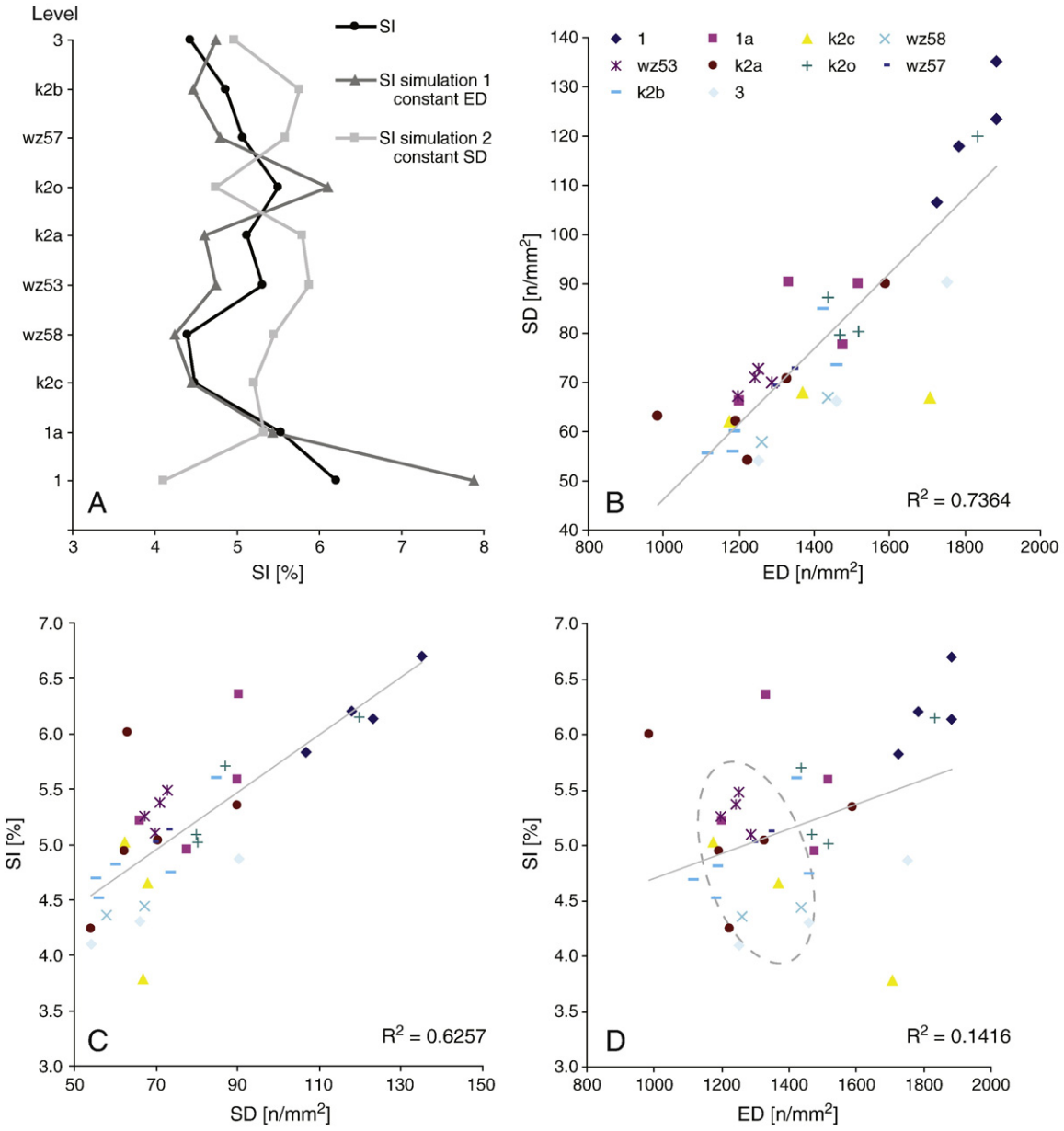

Fig. 9. A) Simulated SI values with a constant ED and a constant SD compared to the original SI values. B) Correlation between SD and ED for each leaf within a fossil level. C) Correlation between SI and SD for each leaf within a fossil level. D) Correlation between SI and ED for each leaf within a fossil level.

Table 3a
Corrected SI of *Lepidopteris ottonis* (SI '*Ginkgoites*') used to reconstruct CO_2 values with the stomatal ratio method. SI '*Ginkgoites*' = SI *Lepidopteris* − 1.95. SR = SI NLE/SI fossil. SI NLE = 11.33%. $CO_{2\ max}$ = SR*600, $CO_{2\ min}$ = SR*360.

Level	SI Lepidopteris	SI Ginkgoites	SI 'Ginkgoites'	SR	$CO_{2\ min}$	$CO_{2\ max}$
3	4.43	2.47		4.58	1649.52	2749.19
k2b	4.87		2.92	3.88	1397.93	2329.89
wz57	5.07		3.12	3.63	1306.43	2177.39
k2o	5.49		3.54	3.20	1152.40	1920.66
k2a	5.11		3.16	3.58	1290.21	2150.35
wz53	5.30		3.35	3.38	1217.51	2029.19
wz58	4.40		2.45	4.63	1666.71	2777.85
k2c	4.49		2.53	4.47	1610.63	2684.38
1a	5.53		3.57	3.17	1141.00	1901.67
1	6.21		4.26	2.66	957.29	1595.49

that, besides CO_2, also volcanogenic SO_2 can have a significant effect on leaf stomata (Tanner et al., 2007). However, at present it is not possible to recognize an SO_2 effect in deep-time leaf records.

Notably, the observed decrease in SI of *Lepidopteris ottonis* (~29%) from the bottom to the top of the Wüstenwelsberg section is consistent in direction with ginkoalean leaf fossil stomatal frequency through late Triassic sediments of East Greenland (McElwain et al., 1999). This makes it plausible that there are indeed global CO_2 changes during the Triassic–Jurassic transition. The reconstructed end-Triassic CO_2 value of between 1650 and 2750 ppmv from Wüstenwelsberg corresponds with the values reconstructed from East Greenland and Sweden, where CO_2 increased from 600 to 2100–2400 ppmv across the Triassic–Jurassic boundary (McElwain et al., 1999). There is palynological evidence that the uppermost sample from the Wüstenwelsberg section is Jurassic in age, which suggests that level 3 correlates with the transition from the *Lepidopteris* zone to the *Thaumatopteris* zone (McElwain et al., 1999, 2007). The present

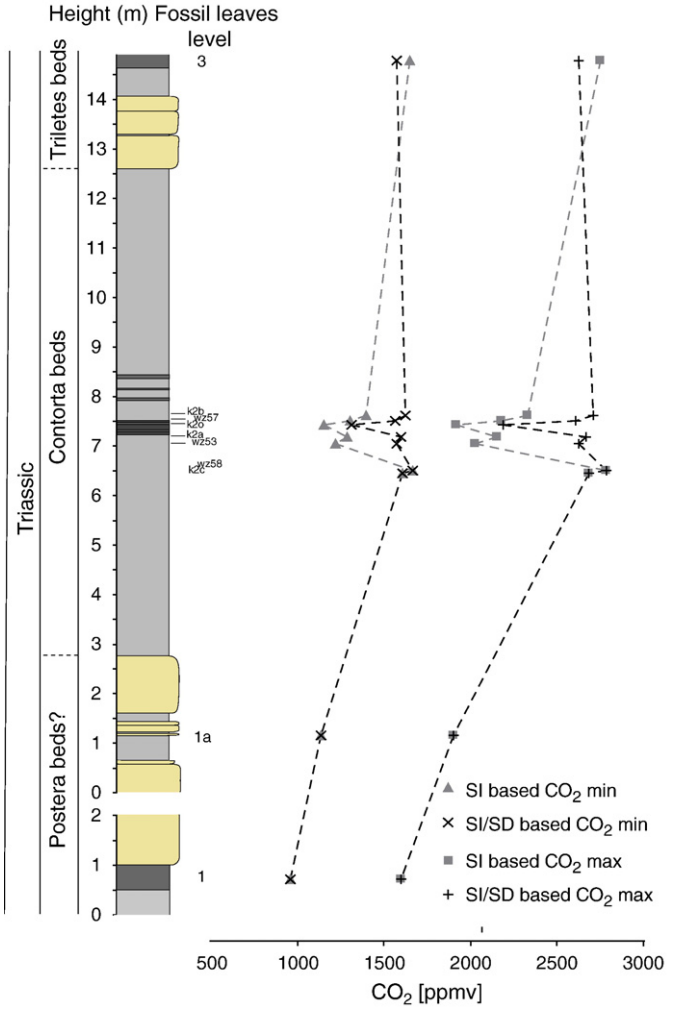

Fig. 10. Reconstruction of atmospheric CO_2 changes in the Wüstenwelsberg section based on the SI value of *Ginkgoites taeniatus* from the uppermost level 3 and on the corrected *Lepidopteris ottonis* SI (SI '*Ginkgoites*,' Table 3a) values from the other levels.

Table 3b
Corrected CO_2 values based on the changes in SD.

Interval	ΔSD	$\Delta CO_{2\ min}$	$\Delta CO_{2\ max}$	% SD change	$\Delta CO_{2\ min}$ new	$\Delta CO_{2\ max}$ new
1 to wz58	58.28	709.42	1182.36			
wz58 to wz53	7.81	449.20	748.66	13.41	95.12	158.53
wz58 to k2a	5.51	376.50	627.50	9.45	67.04	111.73
wz58 to k2o	29.30	514.31	857.19	50.26	356.58	594.30
wz58 to wz57	8.56	360.28	600.46	14.69	104.21	173.69
wz58 to k2b	3.45	268.78	447.97	5.92	41.99	69.98
wz58 to 3	7.65	17.19	28.66	13.12	93.07	155.11

Table 3c
SI/SD based CO_2 values.

Level	$CO_{2\ min}$ new	$CO_{2\ max}$ new
3	1573.64	2622.74
k2b	1624.72	2707.87
wz57	1562.50	2604.16
k2o	1310.13	2183.55
k2a	1599.67	2666.12
wz53	1571.60	2619.33
wz58	1666.71	2777.85
k2c	1610.63	2684.38
1a	1141.00	1901.67
1	957.29	1595.49

study shows that already prior to the Triassic–Jurassic transition CO_2 values were high (Fig. 10). This is in line with the carbon-isotope study on pedogenic carbonate nodules by Cleveland et al. (2008) which shows increased Rhaetian levels (>1500 ppmv) and at least two periods of extreme CO_2 levels (~3000 ppmv) preceding the Triassic–Jurassic boundary. Unfortunately, these North American data lack a detailed chronological resolution so a one-to-one correlation is at present not possible. Furthermore, it is suggested that palaeoatmospheric CO_2 concentrations based on pedogenic carbonates may have been significantly overestimated because the portion of seasonal variability that pedogenic carbonate records is poorly constrained (Breecker et al., 2009).

5. Conclusions

The extinct seed fern *Lepidopteris ottonis* appears to be useful in reconstructing relative CO_2 changes. The intra- and interpinnule variability of the SI is small. Despite the fact that *L. ottonis* shows various xeromorphic features, we suggest this is an adaptation to a stressed (swamp) environment rather than just a dry environment. With the use of co-occurring *Ginkgoites taeniatus* leaves from the youngest fossil level, an elevated CO_2 concentration between 1650 and 2750 ppmv was reconstructed for the Triassic–Jurassic boundary interval. In order to infer CO_2 concentrations from *L. ottonis* in the lower part of the section we made a corrected '*Ginkgoites*' SI and estimated the relative changes in CO_2. A remarkable result is that already before the latest Triassic elevated atmospheric CO_2 concentrations were present, which is in line with a previous carbon-isotope study on pedogenic carbonate nodules. It is important that future work will focus on palaeomagnetic, palynological and chemostratigraphic correlation of the different Triassic–Jurassic boundary sections in- and outside the German Triassic Basin to understand the global pattern of these end-Triassic high CO_2 values.

Acknowledgements

We acknowledge funding from the 'high potential' stimulation program of Utrecht University. We are grateful to Stefan Schmeissner and Günter Dütsch for showing us around in the field, providing us with data from the recovered macroflora and sending us *Lepidopteris ottonis* leaves for cuticular analysis. Martijn Deenen and Micha Ruhl are thanked for their help during the field work. We thank Rike Wagner-Cremer for her help with the stomatal frequency analysis and Henk Visscher for constructive comments on an earlier version of the manuscript. We want to thank the editor and two anonymous reviewers for their useful comments. This is publication number 20100602 of The Netherlands Research School of Sedimentary Geology.

References

Antevs, E., 1914. *Lepidopteris ottonis* (Göpp.) Schimp. and *Antholithus zeilleri* Nath. Kungliger Svenska Vetenskapsakademiens Handlingar 51, 3–17.
Ash, S., 1986. Fossil plants and the Triassic–Jurassic boundary. In: Padian, K. (Ed.), The Beginning of the Age of Dinosaurs: Faunal Change Across the Triassic–Jurassic Boundary. Camebridge University Press, pp. 21–30.
Barbacka, M., 1991. *Lepidopteris ottonis* (Goepp.) Schimp. and *Peltaspermum rotula* Harris from the Rhaetian of Poland. Acta Palaeobotanica 31, 23–47.
Beerling, D.J., 1993. Changes in the stomatal density of *Betula nana* leaves in response to increases in atmospheric carbon dioxide concentration since the late-glacial. Special Papers in Palaeontology 49, 181–187.
Beerling, D.J., 1999. Stomatal density and index: theory and application. In: Jones, T.P., Rowe, N.P. (Eds.), Fossil Plants and Spores: Modern Techniques. Geological Society, London, pp. 251–256.
Beerling, D.J., 2002a. Palaeoclimatology—CO_2 and the end-Triassic mass extinction. Nature 415, 386–387.
Beerling, D.J., 2002b. Low Atmospheric CO_2 Levels during the Permo–Carboniferous Glaciation Inferred from Fossil Lycopsids. Proceedings of the National Academy of Sciences of the United States of America 99, 12,567–12,571.
Beerling, D.J., Berner, R.A., 2002. Biogeochemical constraints on the Triassic–Jurassic boundary carbon cycle event. Global Biogeochemical Cycles 16 (3).

Beerling, D.J., Royer, D.L., 2002a. Fossil plants as indicators of the Phanerozoic global carbon cycle. Annual Review of Earth and Planetary Sciences 30, 527–556.
Beerling, D.J., Royer, D.L., 2002b. Reading a CO_2 signal from fossil stomata. New Phytologist 153, 387–397.
Beerling, D.J., Lomax, B.H., Royer, D.L., Upchurch Jr, G.R., Kump, L.R., 2002. An atmospheric *p*CO2 reconstruction across the Cretaceous–Tertiary boundary from leaf megafossils. Proceedings of the National Academy of Sciences of the United States of America 99, 7836–7840.
Bonis, N.R., Kürschner, W.M., Krystyn, L., 2009. A detailed palynological study of the Triassic–Jurassic transition in key sections of the Eiberg Basin (Northern Calcareous Alps, Austria). Review of Palaeobotany and Palynology 156, 376–400.
Breecker, D.O., Sharp, Z.D., McFadden, L.D., 2009. Seasonal bias in the formation and stable isotopic composition of pedogenic carbonate in modern soils from central New Mexico, USA. Geological Society of America Bulletin 121, 630–640.
Chen, L.I.Q., Li, C.S., Chaloner, W.G., Beerling, D.J., Sun, Q.I.G., Collinson, M.E., Mitchell, P.L., 2001. Assessing the potential for the stomatal characters of extant and fossil Ginkgo leaves to signal atmospheric CO_2 change. American Journal of Botany 88, 1309–1315.
Cleveland, D.M., Nordt, L.C., Dworkin, S.I., Atchley, S.C., 2008. Pedogenic carbonate isotopes as evidence for extreme climatic events preceding the Triassic–Jurassic boundary: implications for the biotic crisis? Geological Society of America Bulletin 120, 1408–1415.
Harris, T.M., 1926. The Rhaetic flora of Scoresby Sound, East Greenland. Meddelelser om Grønland 68, 46–148.
Harris, T.M., 1932. The fossil flora of Scoresby Sound, East Greenland. Meddelelser om Grønland 85, 3–109.
Harris, T.M., 1935. The fossil flora of Scoresby Sound, East Greenland. Meddelelser om Grønland 112, 1–176.
Haworth, M., McElwain, J., 2008. Hot, dry, wet, cold or toxic? Revisiting the ecological significance of leaf and cuticular micromorphology. Palaeogeography, Palaeoclimatology, Palaeoecology 262, 79–90.
Hesselbo, S.P., Robinson, S.A., Surlyk, F., Piasecki, S., 2002. Terrestrial and marine extinction at the Triassic–Jurassic boundary synchronized with major carbon-cycle perturbation: a link to initiation of massive volcanism? Geology 30, 251–254.
Hesselbo, S.P., McRoberts, C.A., Pálfy, J., 2007. Triassic–Jurassic boundary events: problems, progress, possibilities. Palaeogeography, Palaeoclimatology, Palaeoecology 244, 1–10.
Jenkyns, H.C., 2003. Evidence for rapid climate change in the Mesozoic–Palaeogene greenhouse world. Philosophical Transactions of the Royal Society A: Mathematical, Physical and Engineering Sciences 361, 1885–1916.
Kelber, K.-P., Van Konijnenburg-Van Cittert, J.H.A., 1997. A New Rhaetian Flora from the neighbourhood of Coburg (Germany) — Preliminary Results. Meded. Ned. Inst. Toegepaste Geowetenschapen TNO 58, 105–113.
Kerp, H., 1990. The study of fossil gymnosperms by means of cuticular analysis. Palaios 5, 548–569.
Krings, M., Kerp, H., Taylor, T.N., Taylor, E.L., 2003. How Paleozoic vines and lianas got off the ground: on scrambling and climbing Carboniferous–Early Permian Pteridosperms. The Botanical Review 69, 204–224.
Kuerschner, W.M., Bonis, N.R., Krystyn, L., 2007. Carbon-isotope stratigraphy and palynostratigraphy of the Triassic–Jurassic transition in the Tiefengraben section — Northern Calcareous Alps (Austria). Palaeogeography, Palaeoclimatology, Palaeoecology 244, 257–280.
Kürschner, W.M., 1996. Leaf stomata as biosensors of palaeoatmospheric CO_2 levels. PhD thesis, Laboratory of Palaeobotany and Palynology, Utrecht University, 153 pp.
Kürschner, W.M., Van der Burgh, J., Visscher, H., Dilcher, D.L., 1996. Oak leaves as biosensors of late Neogene and early Pleistocene paleoatmospheric CO_2 concentrations. Marine Micropaleontology 27, 299–312.
Kürschner, W.M., Stulen, I., Wagner, F., Kuiper, P.J.C., 1998. Comparison of palaeobotanical observations with experimental data on the leaf anatomy of Durmast oak [*Quercus petraea* (Fagaceae)] in response to environmental change. Annals of Botany 81, 657–664.
Kürschner, W.M., Kvaček, Z., Dilcher, D.L., 2008. The Impact of Miocene Atmospheric Carbon Dioxide Fluctuations on Climate and the Evolution of Terrestrial Ecosystems. Proceedings of the National Academy of Sciences of the United States of America 105, 449–453.
Lundblad, B., 1950. Studies in the Rhaeto–Liassic floras of Sweden. Kungliga Svenska Vetenskapsakademiens Handlingar 1 (8), 1–82.
McElwain, J.C., 1998. Do fossil plants signal palaeoatmospheric CO_2 concentration in the geological past? Philosophical Transactions of the Royal Society of London Series B 353, 83–96.
McElwain, J.C., Chaloner, W.G., 1995. Stomatal density and index of fossil plants track atmospheric carbon dioxide in the Palaeozoic. Annals of Botany 76, 389–395.
McElwain, J.C., Mitchell, F.J.G., Jones, M.B., 1995. Relationship of stomatal density and index of *Salix cinerea* to atmospheric carbon dioxide concentrations in the Holocene. The Holocene 5, 216–219.
McElwain, J.C., Beerling, D.J., Woodward, F.I., 1999. Fossil plants and global warming at the Triassic–Jurassic boundary. Science 285, 1386–1390.
McElwain, J.C., Wade-Murphy, J., Hesselbo, S.P., 2005. Changes in carbon dioxide during an oceanic anoxic event linked to intrusion into Gondwana coals. Nature 435, 479–482.
McElwain, J.C., Popa, M.E., Hesselbo, S.P., Haworth, M., Surlyk, F., 2007. Macroecological responses of terrestrial vegetation to climatic and atmospheric change across the Triassic/Jurassic boundary in East Greenland. Paleobiology 33, 547–573.
Pálfy, J., Demény, A., Haas, J., Hetényi, M., Orchard, M.J., Veto, I., 2001. Carbon isotope anomaly and other geochemical changes at the Triassic–Jurassic boundary from a marine section in Hungary. Geology 29, 1047–1050.
Pott, C., Krings, M., Kerp, H., 2008. The Carnian (Late Triassic) flora from Lunz in Lower Austria: paleoecological considerations. Palaeoworld 17, 172–182.
Retallack, G.J., 2001. A 300-million-year record of atmospheric carbon dioxide from fossil plant cuticles. Nature 411, 287–290.
Retallack, G.J., 2002a. Palaeoclimatology — Triassic–Jurassic atmospheric CO_2 spike. Nature 415, 387–388.
Retallack, G.J., 2002b. *Lepidopteris callipteroides*, an earliest Triassic seed fern of the Sydney Basin, southeastern Australia. Alcheringa 26, 475–500.
Retallack, G.J., 2009. Greenhouse crises of the past 300 million years. Geological Society of America Bulletin 121, 1441–1455.
Roth-Nebelsick, A., 2005. Reconstructing atmospheric carbon dioxide with stomata: possibilities and limitations of a botanical pCO_2-sensor. Trees — Structure and Function 19, 251–265.
Royer, D.L., 2001. Stomatal density and stomatal index as indicators of paleoatmospheric CO_2 concentration. Review of Palaeobotany and Palynology 114, 1–28.
Royer, D.L., 2003. Estimating latest Cretaceous and Tertiary atmospheric CO_2 from stomatal indices. In: Wing, S.L., Gingerich, P.D., Schmitz, B., Tomas, E. (Eds.), Causes and Consequences of Globally Warm Climates in the Early Paleogene, vol. 369. Geological Society of America Special Paper, Boulder, Colorado, pp. 79–93.
Royer, D.L., Wing, S.L., Beerling, D.J., Jolley, D.W., Koch, P.L., Hickey, L.J., Berner, R.A., 2001a. Paleobotanical evidence for near present-day levels of atmospheric CO_2 during part of the tertiary. Science 292, 2310–2313.
Royer, D.L., Berner, R.A., Beerling, D.J., 2001b. Phanerozoic atmospheric CO_2 change: evaluating geochemical and paleobiological approaches. Earth-Science Reviews 54, 349–392.
Ruhl, M., 2010. Carbon cycle changes during the Triassic–Jurassic transition. PhD thesis., Universiteit Utrecht, 151 pp.
Ruhl, M., Kürschner, W.M., Krystyn, L., 2009. Triassic–Jurassic organic carbon isotope stratigraphy of key sections in the western Tethys realm (Austria). Earth and Planetary Science Letters 281, 169–187.
Salisbury, E.J., 1927. On the causes and ecological significance of stomatal frequency, with special reference to the woodland flora. Philosophical Transactions of the Royal Society of London. Series B 216, 1–65.
Schimper, W.P., 1869, 1870. Traité de paléontologie végétale. 1, 2. Paris.
Sun, B.N., Xie, S.P., Yan, D.F., Cong, P.Y., 2008. Fossil plant evidence for Early and Middle Jurassic paleoenvironmental changes in Lanzhou area, Northwest China. Palaeoworld 17, 215–221.
Svensen, H., Planke, S., Polozov, A.G., Schmidbauer, N., Corfu, F., Podladchikov, Y.Y., Jamtveit, B., 2009. Siberian gas venting and the end-Permian environmental crisis. Earth and Planetary Science Letters 277, 490–500.
Tanner, L.H., Hubert, J.F., Coffey, B.P., McInerney, D.P., 2001. Stability of atmospheric CO_2 levels across the Triassic/Jurassic boundary. Nature 411, 675–677.
Tanner, L.H., Smith, D.L., Allan, A., 2007. Stomatal response of swordfern to volcanogenic CO_2 and SO_2 from Kilauea volcano. Geophysical Research Letters 34 (15).
Van der Burgh, J., Visscher, H., Dilcher, D.L., Kürschner, W.M., 1993. Paleoatmospheric signatures in Neogene fossil leaves. Science 260, 1788–1790.
Vörding, B. 2008. Palaeozoic and Mesozoic pteridosperm cuticles as possible proxies for palaeoatmospheric carbon dioxide reconstructions — a methodological approach. PhD thesis, WWU Münster, 208 pp.
Wagner, F., Below, R., De Klerk, P., Dilcher, D.L., Joosten, H., Kürschner, W.M., Visscher, H., 1996. A Natural Experiment on Plant Acclimation: Lifetime Stomatal Frequency Response of an Individual Tree to Annual Atmospheric CO_2 Increase. Proceedings of the National Academy of Sciences of the United States of America 93, 11,705–11,708.
Wagner, F., Bohncke, S.J.P., Dilcher, D.L., Kürschner, W.M., van Geel, B., Visscher, H., 1999. Century-scale shifts in Early Holocene CO_2 concentration. Science 284, 1971–1973.
Wagner, F., Dilcher, D.L., Visscher, H., 2005. Stomatal frequency responses in hardwood swamp vegetation from Florida during a 60-year continuous CO_2 increase. American Journal of Botany 92, 690–695.
Woodward, F.I., 1987. Stomatal numbers are sensitive to increases in CO_2 from pre-industrial levels. Nature 327, 617–618.